PROCEEDINGS, Seventeenth Workshop on Geothermal Reservoir Engineering
Stanford University, Stanford, California, January 29-31, 1992
SGP-TR-141

Model Study of Historical Injection in the Southeast Geysers

D. D. Faulder

Idaho National Engineering Laboratory
P.O. Box 1625
Idaho Falls, ID 83402-2107

ABSTRACT

A three component model study of the historical injection of two wells in the Unit 13 area demonstrates that the recovery of injection derived steam is influenced by the geologic structure of the bottom of the reservoir and the relative location of injection wells. The migration of injectate from the first injection well, located up structure from the second, quenched the area around the second injector before it started operation. While both wells had similar cumulative mass injected, nearly five times more injection derived steam is recovered from the first injector than the second. Sensitivity runs were made to three cases of increasing matrix capillary pressure. The recovery of injection derived steam increases with higher values of capillarity. The interaction of structure at the bottom of the reservoir, injection well locations, and matrix capillarity all influence the recovery efficiency of injectate as steam. The model developed in this study will be used to evaluate injection strategies at The Geysers.

INTRODUCTION

The recent productivity and pressure declines at The Geysers are classic symptoms of reservoir fluid resource depletion. However, even if all the fluid initially in place is produced, over 90% of the usable heat remains in place. Thus, the question of how to extract more of the heat in place arises. One answer is to replace the depleted fluid with increased water injection thereby replenishing the reservoir's working fluid.

If an expanded injection program is to be undertaken it is important to understand how injected fluid behaves. We must be able to confidently model and predict the process of injection, re-vaporization, and production of injection derived steam. Additional insight into this process can be gained by studying historical injection at The Geysers. Water injection began in 1969, originally as a cooling tower waste water disposal and has gradually evolved to an accepted method of replenishing water in depleted portions of the reservoir.

A reservoir model study of the Unit 13 area was conducted with the objectives of modeling historical injection and transport of the injectate, to use the deuterium isotopic shift as a naturally occurring tracer, and to understand the importance of matrix capillary forces in the recovery of injection derived steam. The study goal was to determine how to confidently model injection into a vapor-dominated reservoir.

The Unit 13 study area was chosen for several reasons. It has over 11 years of injection history using two injection wells in the study area, exploitation started at essentially undisturbed conditions, and the reservoir performance is well represented in the literature. The study area is shown in Figure 1.

REVIEW OF APPLICABLE LITERATURE

A review of the geologic literature was conducted to develop a working conceptual geologic model. The top of the reservoir is represented by the top of the steam and the bottom of the reservoir by the top of the felsite. It is recognized the top of felsite is not the bottom of the reservoir for most of The Geysers, however several pieces of evidence suggest this is a good approximation for the Unit 13 area. Micro-seismic data for the C-11 injection area, south of the study area indicates the majority of the liquid injected into the greywacke does not appear to migrate deeply into the felsite (Enedy et al., 1991). Very few wells in the study area have productive steam bearing fractures in the felsite.

Beall (1989) noted the steam bearing fractures in the greywacke show no preferential orientation. However, there are areas of north-northeast enhanced permeability due to southeast-west northwest regional extension, resulting in high angle fractures deep in the reservoir and near the

Work supported by the U.S. Department of Energy, Assistant Secretary of Conservation and Renewable Energy, Office of Utility Technology, under DOE Contract No. DE-AC07-76ID01570.

margins (Beall et al., 1989). Thus, the greywacke can be envisioned to be pervasively fractured with areas of north-south enhanced permeability. Gunderson (1990) noted the matrix porosity was related to two factors; vertical depth and distance above the felsite. The algorithm presented by Williamson (1990) is used to implement this observation.

Past reservoir model studies of The Geysers have typically consisted of field-wide studies with the purpose of predicting overall production rates (Williamson, 1990) or of parametric studies. Parametric studies have been performed to examine sensitivities to initial matrix water saturation and heat flow (Pruess and Narasimhan, 1982), the permeability of the matrix and fractures, grid refinement with depth (Lai and Bodvarsson, 1991), and grid orientation (Pruess, 1991). Petrophysical properties for the study were selected from the above literature. The matrix steam-water relative permeability and capillary pressure behavior have not been measured and reported in the literature to date.

The initial water saturation in the matrix has not been directly measured, however a field-wide study by Williamson (1990) used a value of 82%. This high initial matrix water saturation is consistent with the studies of Pruess and Narasimham (1982) and Pruess (1985). Observed chemical and isotopic gradients of the produced steam in the Southeast Geysers are believed to be due to meteoric recharge entering the reservoir from the southeast (Truesdell et al., 1987). The calculated vapor fraction for the Southeast Geysers from Truesdell et al. indicated that the initial produced steam originated almost entirely from vaporized liquid.

DEUTERIUM TRACER DATA

Two steam condensate injection wells were used in the study area. Injector I1 was the sole injection well at the start operations in May 1980, injecting at an average rate of approximately 350 Klbm/hr through 1984. At that time a second injection well (I2) was used and the total injection volume was split. The injection histories for the two well are shown in Figure 2. The injected condensate is enriched in deuterium relative to the reservoir steam and has been used as a tracer (Beall et al., 1989; Gambil, 1990). The operator has conducted a periodic analysis of deuterium in the producing steam wells to track the movement of injection derived steam in the reservoir. This data set is used as a tracer for the model study. Figure 3 presents an example from Beall et al. (1989) of the contoured deuterium isotopic shift in the study area. Six key production wells were significantly affected by the deuterium shift from these two injectors and are labeled P1 - P6 in Figure 3. Injection derived steam was calculated using the equation presented by Beall et al. (1989).

MODEL FEATURES

A reservoir model of the study area was developed using TETRAD, a simulator which was validated with the Stanford geothermal problem set (Shook and Faulder, 1991). The dual porosity reservoir model uses three water components; 1) initial fluid in place, 2) injectate from I1, and 3) injectate from I2. Separate water components for the two injection wells allows detailed tracking of the injectate and a relative determination of the contribution of each injection well to produced injection derived steam (IDS). The model contains 1650 grid blocks, five vertical layers, and decreasing thickness with depth. The bottom layer is uniformly 75 feet thick. The actual well deviated courses are used, based on the open file records of the California Division of Oil and Gas. Fifteen percent of the matrix rock energy was assigned to the fracture domain. This value is conservative compared to the thirty percent used by Williamson (1990). Conceptually, this could be envisioned as zones of fractured rock or a pervasive micro-fracture network. Petrophysical properties were taken from the literature and are summarized in Table 1. The water-steam fracture and matrix relative permeability are presented in Figure 4. Initially, no capillary pressure was used in the matrix.

The reservoir structure was accounted for by using the top of steam and top of felsite maps presented by Thompson and Gunderson (1989) and by Thompson (1989). These maps were digitized and directly entered into the model. Figure 5 shows north-south and east-west cross-sections through the reservoir model. A key feature to note is the large amount of structural relief on the top and bottom of the reservoir model. The reservoir top has approximately 5000 feet of vertical relief over a distance of 10,000 feet, while the reservoir bottom has approximately 3,000 feet of relief over the same distance.

The study area boundary conditions were initially no-flow, however as the study progressed it became necessary to relax this condition, as explained below. The production and injection wells were placed on rate constraint in order to produce the historical rates from the study area. The production wells were set to produce to a 180 psia wellhead pressure, uncorrected for wellbore friction. Heat flow was set at a uniform vertical flux of 500 mW/m^2, consistent with published data.

MODEL CALIBRATION PROCESS

The model was allowed to equilibrate for 20 years prior to the start of exploitation, allowing steam and water saturations to adjust to a stable heat pipe and establishing a vapor-static pressure gradient. The stabilized model was then run for all exploitation cases. Completion intervals of the wells were adjusted to match the observed drilling steam entries. In the case of multiple steam entries, the dominant entry was chosen on the basis of observed compressor pressure increase during drilling. The well productivity indices (PI) were adjusted to allow the wells to produce the observed rates with the 180 psia wellhead pressure constraint. For those cases with initial rig test data, the indicated PI was used as a starting point. The initial rig test data was found to be very reliable indictor of productivity index.

Constant pressure boundaries declining with time were used on the south and west sides of the model to mimic the effect of offset production due to Unit 16, and Units 18 and 20, respectively. Published pressure histories for adjacent areas were used, (Barker et al., 1990 and Enedy et al., 1990). It was observed the injected fluid would quickly migrate to the bottom of the reservoir and flow to the north and then "puddle". A constant pressure boundary is used on the north boundary to relax the no-flow condition and pressures set to the stabilized pre-exploitation conditions. This northward flow of injectate is not surprising, considering the large amount of structural relief present at the bottom of the reservoir. This structural aspect dominates injectate flow for all cases studied.

Several exploitation runs of 1980 to 1991 production data were made with a uniform permeability structure. Additional data from well testing was used to adjust this case to a fracture permeability from 10 mD to 100 mD, generally increasing to the southeast, (Enedy, 1989b). Evidence for directional permeability was noticed on the isotope shift maps of Beall et al., (1989). Based on the ratio of length to width of the isotope shift contours, directional permeability was set as 3X=Y=Z and is consistent with the geologic model. With these changes, a reasonable pressure match was achieved with this base case. However, the modeled tracer data and implied IDS was low compared to historical conditions.

A sensitivity run was made to an initial matrix water saturation of 42%. The lower initial water saturation results in a similar pressure history as the above case; however, the producing enthalpy achieves superheat with in a few months after the start of exploitation. Enedy (1989a) indicates the wells historically did not begin producing an appreciable degree of superheat until after approximately eight years of production. Thus, the lower saturation case does match the observed production data. Again, for this case the modeled tracer recovery and implied IDS was low.

Finally, a series of sensitivity runs was made to study the effect of capillary pressure. It should be noted actual measurements of the capillary pressure have not been reported in the literature for The Geysers. Thus, a family of generic capillary pressure curves were generated as shown in Figure 6. The capillary pressure at residual water saturation varies by two order of magnitude. A scaling calculation using the Leverett J function and realistic values of permeability and porosity for Geysers reservoir matrix rock indicates capillarity could easily be as high as the upper values presented.

The modeled results for no capillarity (base case) and the three capillarity cases are plotted with the observed deuterium tracer data for well P5 in Figure 7. Well P5 is the nearest producer to the injection plume and is probably least effected by reservoir heterogeneity. As can be noted, the higher values better match the observed trends and magnitude of deuterium tracer recovery. Well P5, nearest to injection well I1 is best matched by the moderate to strong capillary pressure function. Figures 8 and 9 present the modeled injection derived steam rate history for the key production wells and the total study area. It can be noted that with increasing capillarity, the injection derived steam increases. This suggests that detailed injection modeling at The Geysers must include matrix capillarity to accurately predict the recovery of injection derived steam.

DISCUSSION OF RESULTS

The simulation results demonstrate that the recovery of injection derived steam is primarily influenced by two factors. First, the structure of the bottom of the reservoir greatly influences injectate movement. This is apparent by the migration of the injectate down the structure. It should be noted that I2 is located lower structurally from I1. When I2 began injection operations, injectate from I1 had already moved down structure, quenching this area. This resulted in low injection derived steam recovery from I2 relative to I1. Secondly, the presence of capillarity increases the recovery of injection derived steam for both wells. Table 2 presents the percent recovery of injection derived steam from each injection well. While each injection well has similar cumulative mass injected, nearly 5 times more injection derived steam is recovered from I1 compared to I2, with injection derived steam

recovery increasing with capillarity. The interaction between structure at the bottom of the reservoir, injection well location, and capillarity all influence the recovery of injection derived steam. Given the geologic structure of the bottom of the reservoir and the ability to select injection well locations, it should be possible to design and model an effective injection program.

The model developed in this study will be used to evaluate injection strategies at The Geysers. Several strategies that will be evaluated include injectate recovery sensitivity to injection rate, a more distributed injection approach, the injectate recovery efficiency of a horizontal injection well, and the selection of injection well locations to allow for reservoir structure.

CONCLUSIONS

The recovery of injection derived steam in the Unit I3 study area has had mixed results. The location of injection well I2 was less than optimally located to maximize the injectate recovery. The strong capillarity case had a total recovery of approximately 30% of cumulative mass injected.

The structure of the bottom of the reservoir can exert a great deal of influence of the direction the injectate travels. It would seem prudent to locate injection wells with this structural aspect in mind.

Modeled injection derived steam recovery is greatly influenced by matrix capillary pressure. Higher values of capillarity result in increased recovery of injection derived steam. Predictive injection modeling at The Geysers will need to consider capillary pressure effects.

The interaction between structure at the bottom of the reservoir, well locations, and capillarity all influence the recovery of injection derived steam.

The measurement of Geysers core and the determination of the actual shape of the capillary pressure curve would enhance our ability to model and predict reservoir response to injection at The Geysers. There is a need to measure the capillary pressure of actual Geysers core to determine the character and magnitude of this effect.

ACKNOWLEDGEMENTS

I would like to thank Dr. Keshav Goyal and Tom Box of Calpine Corporation for providing study data. Their assistance and cooperation are greatly appreciated.

NOMENCLATURE

k_{rg} = relative permeability of gas

k_{rl} = relative permeability of liquid

P_c = capillary pressure

P_c = capillary pressure curve parameter

P_{entry} = capillary entry pressure

S = dimensionless liquid saturation

S_{gc} = critical gas saturation

S_{ir} = irreducible liquid saturation

S_l = liquid saturation

REFERENCES

Barker, B. J., M. S. Gulati, M. A. Bryan, and K. L. Riedel; 1989; Geysers Reservoir Performance; **Trans.** Geothermal Resources Council, Vol. 13.

Beall, Joseph J., Steve Enedy, and W. T. Box, Jr.; 1989; Recovery of Condensate as Steam in the South Geysers Field; **Trans.** Geothermal Resources Council, Vol. 13, p. 351-357.

Beall, Joseph J. and W. T. Box, Jr.; 1989; The Nature of Steam Bearing Fractures in the South Geysers Reservoir; **Trans.** Geothermal Resources Council, Vol. 13, p. 441-448.

Enedy, Steve, Murray Grande, and J. L. Bill Smith; 1990; A Case History of Steamfield Development, Reservoir Evaluation, and Power Generation in the Southeast Geysers; Geothermal Resources Council *Bulletin*, Oct., p. 232-248.

Enedy, Kathleen L., 1989a; Downhole Enthalpy and Superheat Evolution of Geysers Steam Wells; **Trans.** Geothermal Resources Council, Vol. 13, p. 377-382.

Enedy, Kathleen L., 1989b; The Role of Decline Curve Analysis at The Geysers; **Trans.** Geothermal Resources Council, Vol. 13, p. 383-391.

Enedy, Steven, Kathy Enedy, and John Maney, 1991; Reservoir Response to Injection in the Southeast Geysers, **Proc.** 16th Workshop on Geothermal Reservoir Engineering, Stanford Univ., in press.

Gambil, David T.; 1990; The Recovery of Injected Water as Steam at The Geysers; Trans. Geothermal Resources Council, Vol. 14, Part II, p. 1655-1660.

Gunderson, Richard P.; 1990; Reservoir Matrix Porosity at The Geysers From Core Measurements; **Trans.** Geothermal Resources Council, Vol. 14, Part II, p. 1661-1665.

Lai, C. H. and G. S. Bodvarsson; 1991; Numerical Studies of Cold Water Injection into Vapor-Dominated Geothermal Systems, LBL-30173, 26 p.

Pruess, Karsten; 1985; A Quantitative Model of Vapor Dominated Geothermal Reservoirs as Heat Pipes in Fractured Porous Rock; **Trans.** Geothermal Resources Council, Vol. 9, Part II, p. 353-361.

Pruess, K. and T. N. Narasimhan; 1982; On Fluid Reserves and the Production of Superheated Steam From Fractured, Vapor-Dominated Geothermal Reservoirs, *J. Geophys. Res.*, Vol 87(B11), p. 9329-9339.

Shook, Mike and D. D. Faulder; 1991; Validation of a Geothermal Simulator, EGG-EP-9851.

Stockton, A. D., R. P. Thomas, R. H. Chapman, and Herman Dykstra; 1983; A Reservoir Assessment of The Geysers Geothermal Field, SPE 11727.

Thompson, Richard C.; 1989; Structural Stratigraphy and Intrusive Rocks at The Geysers Geothermal Field, **Trans.** Geothermal Resources Council, Vol. 13, p. 481-485.

Thompson, Randolph C. and Richard P Gunderson; 1989; The Orientation of Steam-Bearing Fractures at The Geysers Geothermal Field; **Trans.** Geothermal Resources Council, Vol. 13, p. 487-490.

Truesdell, A. H., J. R. Haizlip, W. T. Box, Jr., and F. D'Amore; 1987; Fieldwide Chemical and Isotopic Gradients in Steam from The Geysers; **Proc.** 12th Workshop on Geothermal Reservoir Engineering, Stanford Univ., p. 241-246.

Williamson, K. H.; 1990; Reservoir Simulation of The Geysers Geothermal Field; **Proc.** 15th Workshop on Geothermal Reservoir Engineering, Stanford Univ., p. 113-123.

Table 1

Petrophysical Properties

Porosity

matrix	4.6% - 2.96%	decreasing with depth
fracture	2.0% - 1.45%	decreasing with depth

Permeability

matrix	10 micro Darcy	uniform
fracture	10 to 100 mD	varying

Fracture Spacing

150 feet

Relative Permeability

matrix — Corey type, with Sir = 30%, Sgc = 5%

$$k_{rl} = (S)^4 \qquad k_{rg} = (1 - S)^{2.5} \qquad S = \left(\frac{S_l - S_{ir}}{1 - S_{ir} - S_{gc}}\right)$$

fracture — straight line X curves, no residual saturations

$$k_{rl} = S_l \qquad k_{rg} = \left(1 - S_l\right)$$

Initial Water Saturations

matrix	Sw=82%
fracture	Sw=.04%

Capillary Pressure

matrix $\qquad P_c = \dot{P}_c(1 - S)^2 + P_{entry}$

Heat Flow

500 mW/m^2 top and bottom of model

Rock Thermal Properties

density	170 lbm/ft^3
specific heat	.21 BTU/lbm - F
thermal conductivity	33.3 BTU/ft- F-day

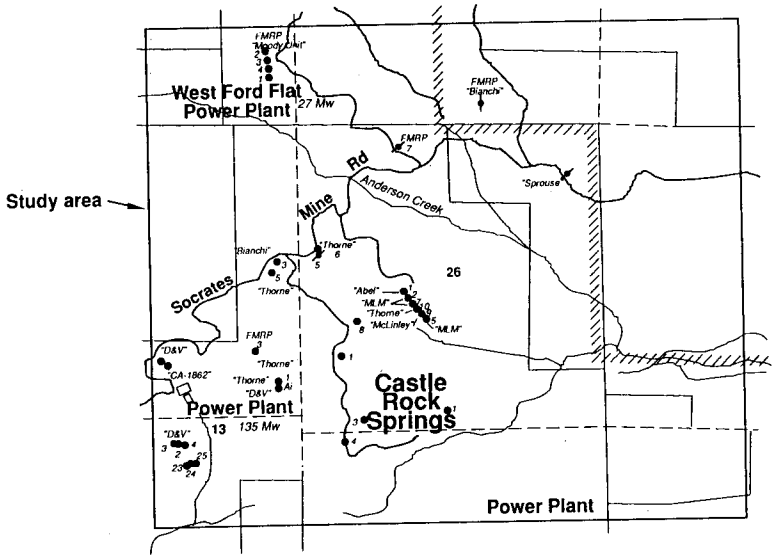

Figure 1 Study Area

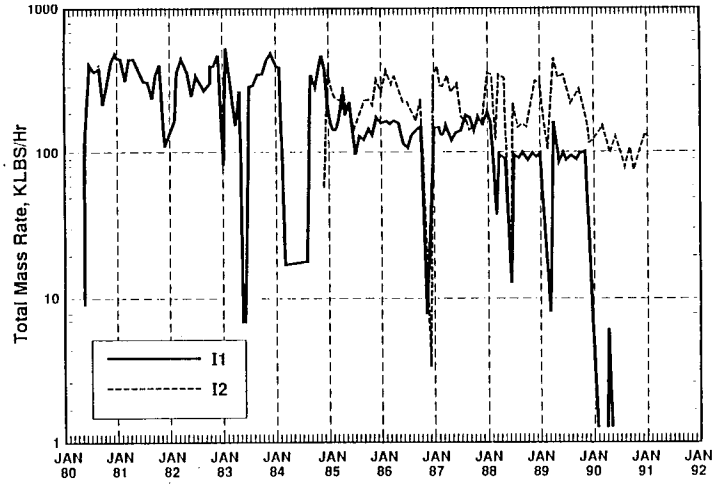

Figure 2 Historical Injection Rates for I1 and I2

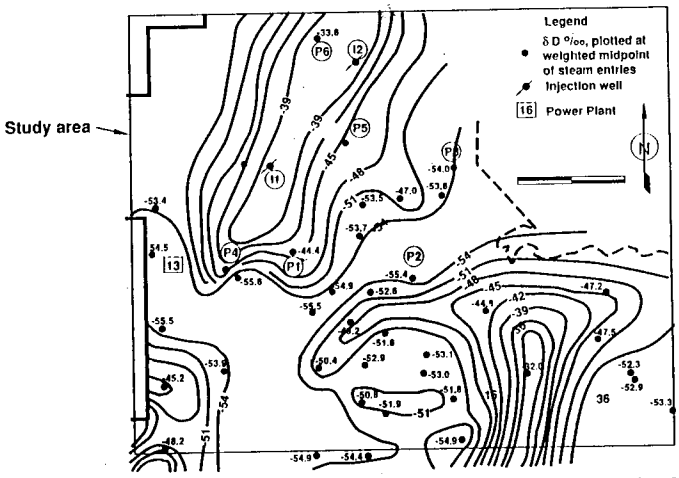

Figure 3 Deuterium Isotopic Shift for Study Area, modified from Beall, Enedy, and Box, 1989.

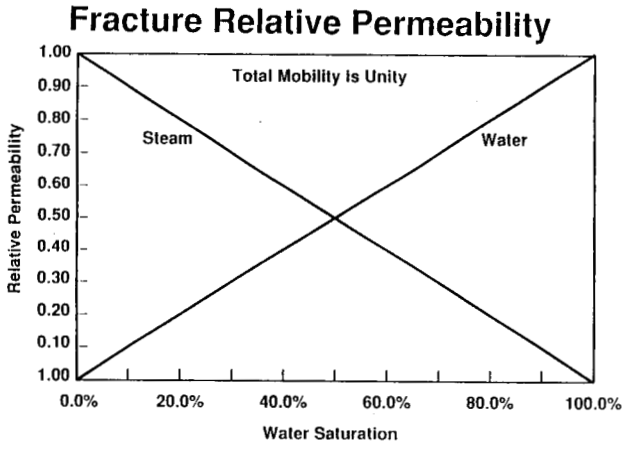

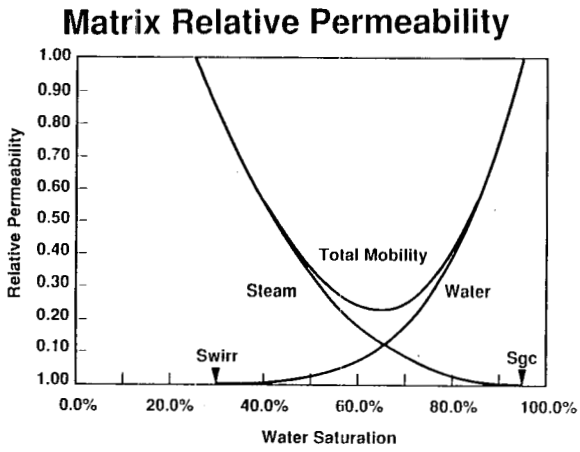

Figure 4 Fracture and Matrix Relative Permeability Curves

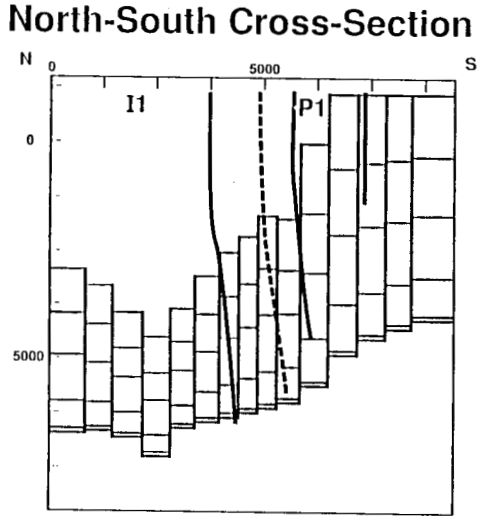

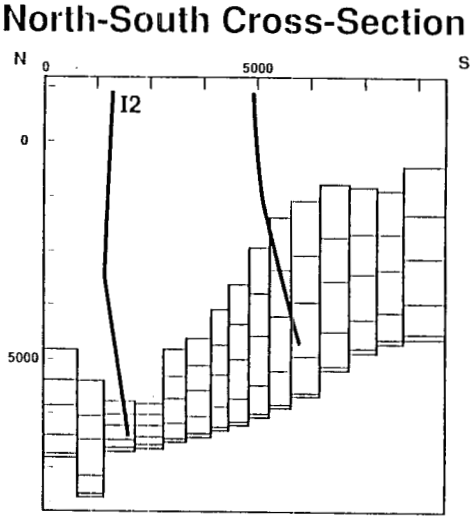

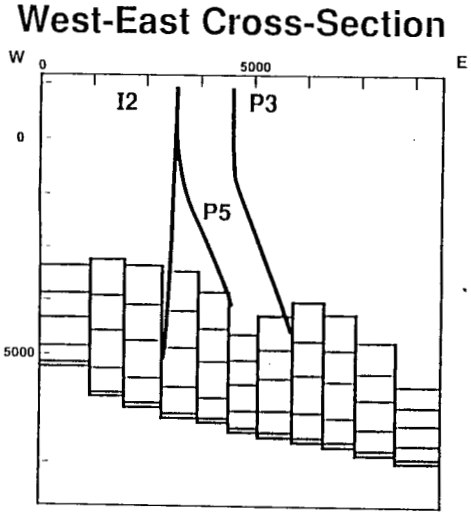

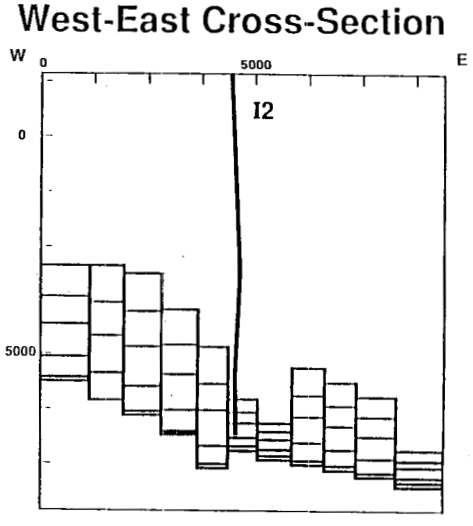

Figure 5 Select Cross-Sections of the Model

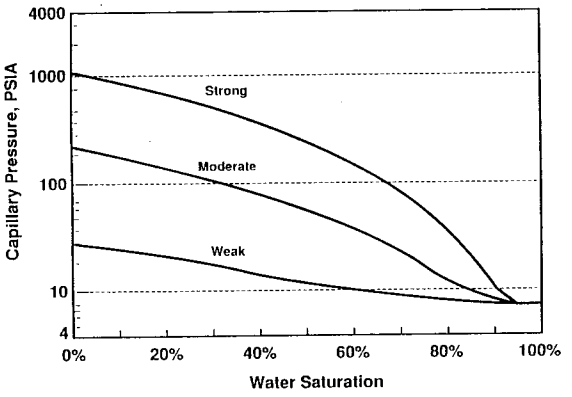

Figure 6 Matrix Capillary Pressure

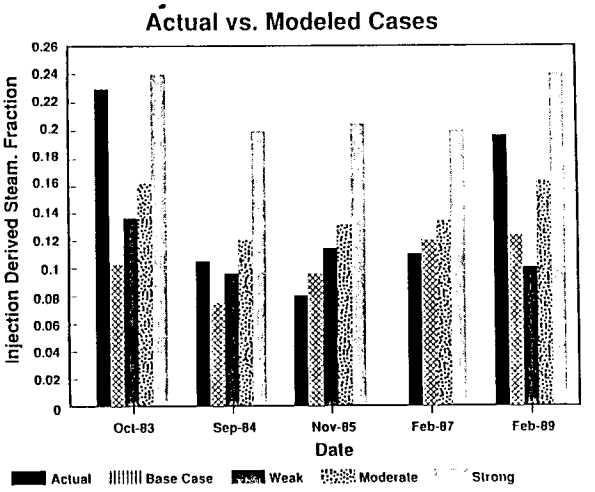

Figure 7 Injection Derived Steam Results for Well P5

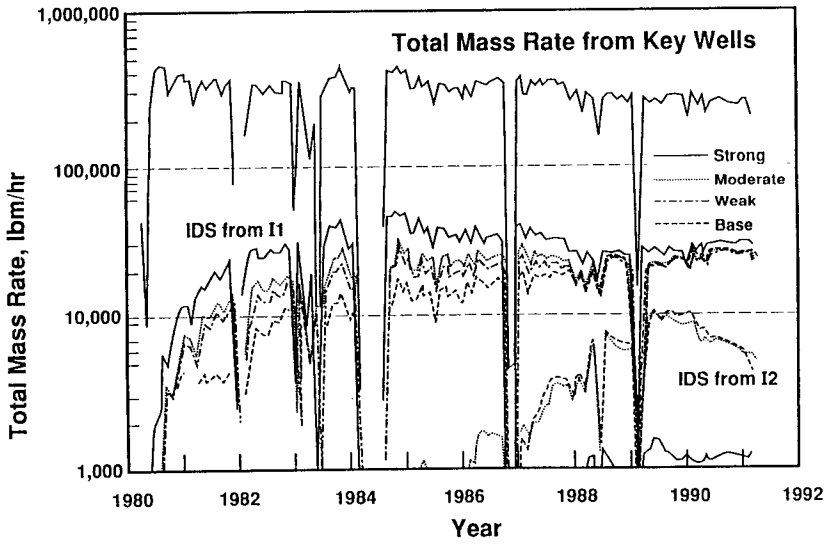

Figure 8 Key Wells Modeled Injection Derived Steam

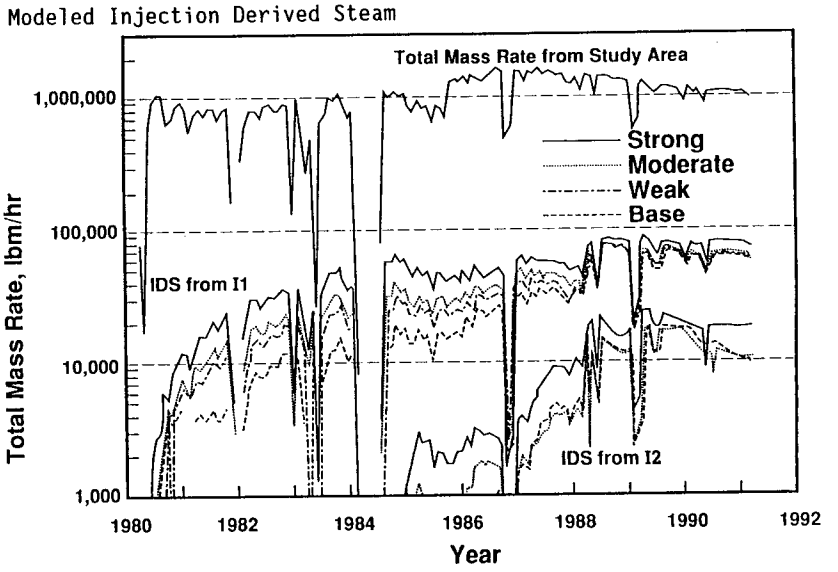

Figure 9 Study Area Modeled Injection Derived Steam

Table 2

Recovery of Injection Derived Steam

Cumulative Injection into I1 1.75E+7 Klbm
Cumulative Injection into I2 1.18E+7 Klbm

Key Wells

Case	% Recovery from I1	% Recovery from I2
Base	7.1	1.9
Weak Capillarity	8.5	1.7
Moderate Capillarity	9.5	1.9
Strong Capillarity	13.2	3.0

Total Study Area

Case	% Recovery from I1	% Recovery from I2
Base	14.5	3.3
Weak Capillarity	16.7	3.1
Moderate Capillarity	18.3	3.3
Strong Capillarity	24.1	5.0